Quantum simulation for peak broadening in atom lithography

Min Zhao (赵 敏), Zhanshan Wang (王占山), Yan Ma (马 艳), Bin Ma (马 彬), and Fosheng Li (李佛生)

Institute of Precision Optical Engineering, Department of Physics, Tongji University, Shanghai 200092

Received April 23, 2007

A grating structure with period of half of the laser wavelength generated by focusing Cr atoms with nearly resonant laser standing wave atom lens was simulated using a quantum-mechanical model. The influence of thermal atomic source on atom focusing, including the statistical distribution of the longitudinal velocity and the beam divergence, was discussed. The background and full-width at half-maximum (FWHM) of atomic density peaks with v_z in Maxwell distribution and v_{x0} in Gaussian distribution increase significantly compared with ideal atoms. Collimating atoms with laser cooling is necessary to decrease the peak broadening.

OCIS codes: 020.0020, 260.0260, 270.0270.

Evolving from the initial experiments with Na[1] and Cr atoms[2] ten years ago, the study of atom lithography using standing wave (SW) light fields has developed into a broad area of research in atom optics during the latest years[3−6]. Compared with conventional lithography techniques, the SW field can act as an array of optical lenses to focus atoms into periodic lines or dots during depositing onto a substrate. Since real atoms in the experiments will deviate from the ideal focusing plane and bring peak broadening, it is necessary to discuss how the focusing results are influenced. Particle optics approach[7−9] has been used to simulate atom deposition in SW. However, this method can only make rough estimate, since it neglects the wave nature of atoms. In order to get the influence of various practical experimental conditions on peak broadening in detail, it is very necessary to use quantum approach, which has not been discussed thoroughly[10]. In this paper, we discuss the influence of Cr atomic source on atom focusing, including the statistical distribution of atom longitudinal velocity and the atom beam divergence, with quantum mechanical approach.

In our simulation, it is assumed that the Cr atoms move along the z direction with v_z and the laser SW applies along the x direction. Since the laser intensity reaches peak value at the Gaussian beam center $z = z_0 = 1.5\omega_0$, and drops sharply to 1% of the peak value when departing from $z = z_0$ to $z = z_0 \pm 1.5\omega_0$[10], we take $3\omega_0$ as the longitudinal interaction length. The intensity of SW can be written as[10]

$$I(x,t) = I_{\max} \exp[-2\frac{(z-1.5\omega_0)^2}{\omega_0^2}] \cos^2[k(x-\lambda/4)], \quad (1)$$

where $I_{\max}$, ω_0, λ are the maximal light intensity, $1/e^2$ radius of SW at the beam waist, the wavelength of laser field, respectively. When laser SW frequency is detuned close to the atomic resonance $^7S_3 \rightarrow {}^7P_4^0$, a periodical potential field on atoms is generated which takes the form[10]

$$V(x,t) = \frac{\hbar\Delta}{2}\{1 + \frac{\Omega_{\max}^2}{\Delta^2} \exp[-2\frac{(v_z t - 1.5\omega_0)^2}{\omega_0^2}] \times \cos^2[k(x-\lambda/4)]\}^{1/2}, \quad (2)$$

where $\Omega_{\max}$, $\Delta = \omega - \omega_A$ are the peak Rabi frequency, the detuning between the laser frequency and the atomic transition frequency, respectively. Here we take $z = v_z t$ because the force on atoms along the z direction is 10^{-6} times of that along the x direction, thus the velocity of atoms along the z direction may be treated unchanged. The minimum potential value appears at wave nodes $x = 2n\lambda/4$ when the laser field is blue-detuned. The dynamics of a two-level atom can be described by the time dependent on Schrödinger equation[10]

$$i\hbar\frac{\partial}{\partial t}\Psi_g(x,t) = [\frac{p_x^2}{2m} + \hbar\frac{\Delta}{2} + V(x,t)]\Psi_g(x,t). \quad (3)$$

We propagate the solution of Eq. (3) through the z direction using Crank-Nicolson[11] method of numerical integration and start the calculation with $\lambda = 425.55$ nm, $\Delta = +200$ MHz, $v_z = 926$ m/s, $\omega_0 = 195$ μm, $\Omega_{\max} = 0.564 \times 10^9$ Hz. The boundary condition is $0 \le z \le 3.0\omega_0$ and the initial wave function is equal in the x direction. The results of wave mechanical simulation with ideal atoms are shown in Fig. 1. Here ideal atoms mean atoms with mono-longitudinal velocity v_z and without beam divergence. In Fig. 1(a), it is obvious that the atomic density reaches maximum at the wave nodes $x = 2n\lambda/4$ in transverse direction and at the Gaussian center $z = z_0$ of the SW in longitudinal direction. In Fig. 1(b), it shows that the feature contrast at the Gaussian center is about 15:1 and the full width at half maximum (FWHM) is 5.3 nm. The background arises because not all the atoms within $x \in [-\lambda/4, +\lambda/4]$ focus at the same z position. Atoms far from the potential minimum (which occur at wave nodes) endure smaller force, thus need longer propagation distances z before being focused[12].

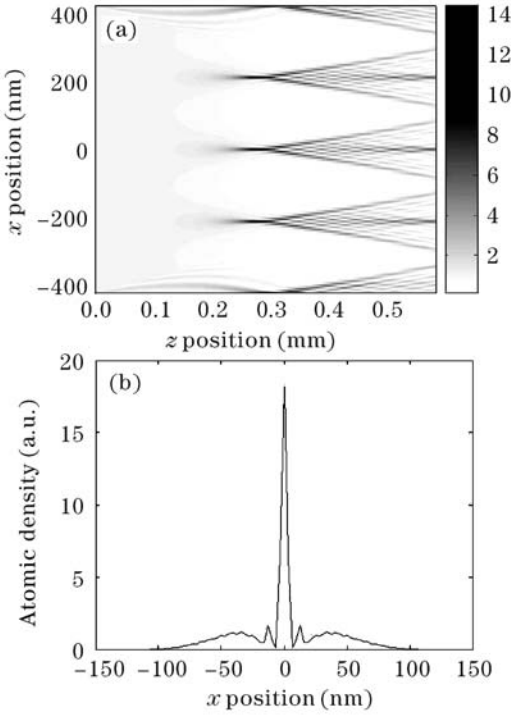

Fig. 1. Density distribution for Cr atoms with mono-longitudinal velocity $v_z = 926$ m/s and without beam divergence. (a) Density distribution for coherent evolution in the SW (black color corresponds to maximum atomic intensity); (b) atomic density at the focal plane $z = z_f$.

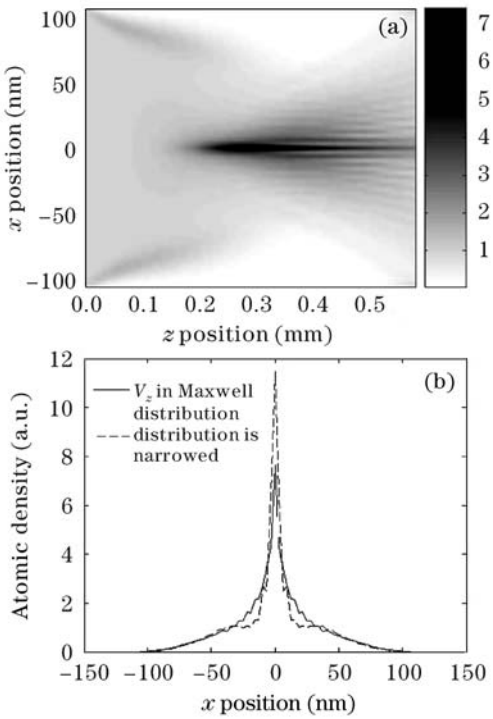

Fig. 2. (a) Density distribution for Cr atoms with v_z in Maxwell distribution. $v_{zp} = 926$ m/s. Beam divergence is not considered. (b) Density distribution at the focal plane $z = z_f$. Solid line is for the full range of velocities, dashed line is for velocities from $0.6v_{zp}$ to $1.4v_{zp}$.

In the experiments the atoms are usually emitted from an oven operating at a relatively high temperature. Therefore, mono-energetic beams are not feasible. The longitudinal velocity of atoms emitted from the oven at temperature T obeys Maxwell distribution represented by[9]

$$f(v_z) = \frac{1}{2}(\frac{m}{k_B T})^2 v_z^3 \exp(-\frac{m v_z^2}{2k_B T}), \tag{4}$$

where k_B is Boltzmann constant.

Supposing that beam divergence is zero, the effect of Maxwell distribution of v_z is shown in Fig. 2, where the most probable speed v_{zp} is 926 m/s. Different v_z leads to different atomic density distributions. To obtain the final result these individual distributions are averaged with weighting factors depicted in Eq. (4). Figure 2(a) shows that the focal depth is longer than that for ideal atoms (see Fig. 1(a)), which indicates that the position of substrate for atoms with v_z in Maxwell distribution is not as strict as for ideal atoms. The focal depth extends because the atoms with various v_z undergo the interaction for differing times and therefore become focused at different distances. In Fig. 2(b), the FWHM with v_z in Maxwell distribution increases to 10 nm at the focal plane $z = z_f$ compared with 5.3 nm in Fig. 1(b). The contrast decreases to 8:1 and the background increases obviously. It is because the atoms with various v_z focus at different distances, therefore, they do not arrive at the minimum potential at the same longitudinal distance. Figure 2(b) also shows that the FWHM does not decrease much when the spread in v_z is narrowed, but the peak value increases greatly.

The initial transverse velocity v_{x0} of thermal atoms is normally not 0, but is assumed to exhibit a Gaussian spread[9]

$$f(v_{x0}) = (\frac{m}{2\pi k_B T_c})^{1/2} \exp(-\frac{m v_{x0}^2}{2k_B T_c}), \tag{5}$$

where $T_c = T \cdot (2\overline{v_{x0p}}/v_z)^2/4(\sqrt{2}-1)$ is the transverse temperature of the atom beam. Here $\overline{v_{x0p}} = \alpha \cdot v_z/2$, where α is the FWHM divergence angle. Different v_{x0} leads to different initial wave function $\Psi(x, t = 0) \sim \exp(i\overrightarrow{k_{0x}}x)$ and therefore different atomic distributions. To obtain the final result these individual distributions are averaged with weighting factors depicted in Eq. (5). The effect of T_c with mono-longitudinal velocity $v_z = 926$ m/s is given in Fig. 3, which shows that FWHM increases

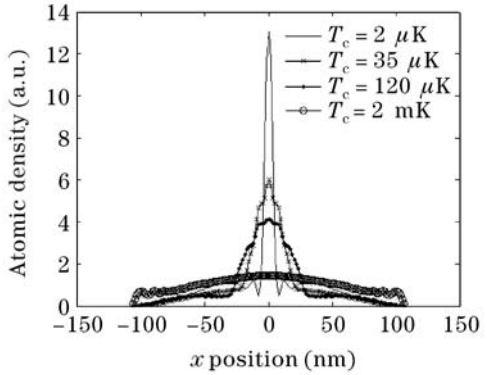

Fig. 3. Atomic distribution at the focal plane $z = z_f$ under various T_c, $T_c = 2$ μK, 35 μK, 120 μK, 2 mK. Mono-longitudinal velocity $v_z = 926$ m/s.

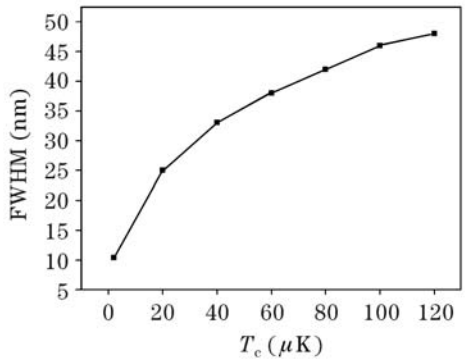

Fig. 4. Atomic distribution for various T_c, Maxwellian longitudinal velocity $v_{zp} = 926$ m/s.

with T_c obviously. The FWHMs are 7.3, 24, 46, 167 nm when T_c are 2 μK, 35 μK, 120 μK, 2 mK, respectively. The deposition curve is almost plane when $T_c = 2$ mk, which means that the density peak will disappear if atoms are not collimated in the x direction beforehand. Thus we can conclude that it is very necessary to decrease the atom beam divergence α to obtain a good focusing performance. In order to get a small α, the atoms are usually collimated with laser cooling. Normally, the temperature limit of Cr atoms is 120 μK for Doppler cooling and much smaller for sub-Doppler cooling, such as Sisyphus cooling, velocity-selective coherent population trapping, and Raman cooling[13].

The best Cr deposition results were given by Ref. [14] with FWHM of 38 nm. To find out the feasible condition for such small FWHM, the relationship between FWHM and thermal atoms with various T_c is discussed in Fig. 4. It shows that when $v_{zp} = 926$ m/s and $T_c = 60$ μK, the FWHM decreases to 38 nm. If T_c becomes smaller, density peak will be sharper. We also find that the position of the focal plane and the peak value are influenced by Δ, v_z, ω_0, and Ω_{max}. We will discuss these factors in other manuscripts.

In summary, we deduced the Schrodinger equation of an atom-SW system using the quantum mechanical method. How the real thermal atom source influences the atomic motion was discussed. It was found that the background and FWHM of thermal atom density peaks with v_z in Maxwell distribution and v_{x0} in Gaussian distribution increase significantly compared with ideal atoms. Since atoms with different v_z focus at different longitudinal distances, the position of substrate in the atomic optics experiments is not as strict as that for ideal atoms. The influence of v_{x0} on atomic deposition is so big that the density peak will disappear if atoms are not cooled beforehand. The model we developed will serve as a valuable guide for further experiments.

This work was supported by the Nanoscience Foundation of Shanghai under Grant No. 0259nm034 and 0452nm029. M. Zhao's e-mail address is minminzhao@mail.tongji.edu.cn.

References

1. G. L. Timp, R. E. Behringer, D. M. Tennant, J. E. Cunningham, M. Prentiss, and K. K. Berggren, Phys. Rev. Lett. **69,** 1636 (1992).
2. J. J. McClelland, R. E. Scholten, E. C. Palm, and R. J. Celotta, Science **262,** 877 (1993).
3. R. W. McGowan, D. M. Giltner, and S. A. Lee, Opt. Lett. **20,** 2535 (1995).
4. F. Lison, H.-J. Adams, D. Haubrich, M. Kreis, S. Nowak, and K. Meschede, Appl. Phys. B **65,** 419 (1997).
5. K. S. Johnson, J. H. Thywissen, N. H. Dekker, K. K. Berggren, A. P. Chu, R. Younkin, and M. Prentiss, Science **280,** 1583 (1998).
6. P. Engels, S. Salewski, H. Levsen, K. Sengstock, and W. Ertmer, Appl. Phys. B **69,** 407 (1999).
7. J. J. McClelland, J. Opt. Soc. Am. B **12,** 1761 (1995).
8. X. Chen, H. Yao, and X. Chen, Chin. Opt. Lett. **2,** 187 (2004).
9. B. Ma, Y. Ma, M. Zhao, S. Ma, and Z. Wang, Acta Phys. Sin. (in Chinese) **55,** 667 (2006).
10. C. J. Lee, Phys. Rev. A **61,** 063604 (2000).
11. W. H. Press, S. A. Teukolsky, W. T. Vetterling, and B. P. Flannery, *Numerical Recipes in C* (Cambridge University Press, Cambridge, 1992) p.853.
12. K. K. Berggren, M. Prentiss, G. L. Timp, and R. E. Behringer, J. Opt. Soc. Am. B **11,** 1166 (1994).
13. W. Cai, C. Li, Y. Huo, and Y. Wang, Acta Phys. Sin. (in Chinese) **48,** 611 (1999).
14. R. J. Celotta, R. Gupta, R. E. Scholten, and J. J. McClelland, J. Appl. Phys. **79,** 6079 (1996).